Stand-alone island daily power management using a tidal turbine farm and an ocean compressed air energy storage system

L. Sheng [a], Z. Zhou [b, *], J.F. Charpentier [b], M.E.H. Benbouzid [c, d]

[a] Huazhong University of Science and Technology, Wuhan, China
[b] French Naval Academy, EA 3634 IRENav, 29240 Brest Cedex 9, France
[c] University of Brest, FRE CNRS 3744 IRDL, 29238 Brest Cedex 03, France
[d] Shanghai Maritime University, 201306 Shanghai, China

A B S T R A C T

Due to the high predictability and the high energy density, marine tidal resource has become an area of increasing interest with various academic and industrial projects around the world. In fact, several Marine Current Turbine (MCT) farm projects with multi-megawatt capacity are planned to be installed in the coming years. In this paper, a MCT farm is supposed to be the main energy supply for a stand-alone island. To compensate the MCT farm power variation relating to the tidal phenomenon, an Ocean Compressed Air Energy Storage (OCAES) system is considered to achieve the island power management. The novelty in this work is that conventional Diesel Generators (DGs) would only serve as a backup supply while the main island power supply will be fulfilled by the proposed hybrid MCT/OCAES system. A simplified OCAES model is built-up in this paper with cycle efficiency about 60.6%. Simulations under different working conditions are carried out to validate the feasibility of the hybrid power system. The obtained results show that the proposed system power management can greatly help to decrease DG fossil fuel consumption and CO_2 emission.

Keywords:
Tidal energy
Marine current turbine
Island power supply
Compressed air energy storage

1. Introduction

Intense energy density and high predictability of tidal current resources make marine current turbine (MCT) a promising technology for generating electricity from the oceans. Industrial and academic research progresses on the MCT turbine designs are presented in Ref. [1]. Several megawatt level systems are currently under test and planned to be installed in pilot MCT farms in the coming years [2]. Similar to a wind turbine, the total kinetic power harnessed by a marine current turbine can be calculated by (1),

$$P = \frac{1}{2} C_p \rho A V^3 \tag{1}$$

Typical turbine power coefficient C_p values for a marine current turbine are in the range of 0.35–0.5 [3]. Different from wind turbines, MCT works in the seawater being more corrosive than air. Decreasing maintenances of MCTs as low as possible is required. Eliminating pitch control can be an interesting design option for MCTs because this system increases system complexity with high maintenance requirements [4].

Power variation is still a problem for MCTs. For a daily-time scale, the astronomic nature of tides causes seawater to flow regularly each day (flood and ebb tides). For a longer time scale, the amplitude of the tide varies with the relative position of earth, moon and sun (spring and neap tides). On the other hand, an island grid load has its own variation pattern each day, which is related to the consumer's behavior. Therefore, the energy storage system (ESS) is essential to solve the unbalances between the MCT generated power and the local load demand. A detailed comparison and evaluation of different ESS technologies for MCT application can be found in Ref. [5]. Daily power management for a single megawatt MCT based on battery storage system has been studied in Ref. [6].

It is practical to associate several MCTs in an offshore farm to increase the capability of the power generation and to share some common equipment (substation, power line, etc.) [7]. This would be also true in power supply cases of stand-alone islands using a MCT farm. The power demand of some stand-alone islands in Western Europe is generally at several-megawatts level [8]. Some of these islands are located at the vicinity of high tidal current energy potential areas. This is why MCT farm can be an interesting solution to

* Corresponding author.
E-mail address: zhibin.zhou26@gmail.com (Z. Zhou).

Nomenclature

CAES	Compressed air energy storage
DG	Diesel generator
ESS	Energy storage system
PMSG	Permanent-magnet synchronous generator
HTF	Heat transfer fluid
MCT	Marine current turbine
MPPT	Maximum power point tracking
OCAES	Ocean compressed air energy storage
SoC	State of charge
TES	Thermal energy storage frequency component *i*
A	Turbine blade swept area
C_p	Turbine power coefficient
P	Turbine produced power
P_{com}	Compressor consumed power
P_{tur}	Air turbine produced power
Q_{charge}	Heat flux of the TES during charging
$Q_{discharge}$	Heat flux of the TES during charging
R_a	Ideal air mass constant
T	Air temperature
$T_{ambient}$	Ambient air temperature
T_{out}, T_{in}	Outlet and inlet air temperature
T_{ci}, T_{ti}	Air temperature in the compressor and the air turbine
V	Tidal current velocity
$c_{p,a}$	Specific heat capacity of the air
$c_{p,TES}$	Specific heat capacity of the TES
i	Stage i of the compressor/air turbine
m_{air}	Air mass
$m_{c,a}$, $m_{t,a}$	Air mass in the compressor and air turbine
n	Polytropic index
p, p_0	Air pressure and the initial value
t_{charge}	Time duration of charging
$t_{discharge}$	Time duration of discharging
β_i	Pressure ratio of stage i
β_{ci}, β_{ti}	Pressure ratio of stage i in the compressor and air turbine
ρ	Seawater density
$\eta_{m,c}$, $\eta_{m,t}$	Mechanical efficiency of the compressor and the air turbine
η_{global}	Global efficiency of the OCAES
η_{heat}	Heat recycle efficiency of the TES

provide electricity for these islands. In addition, as shown in Fig. 1 from Ref. [9], CAES has lowest costs among other ESSs. Therefore, concerning the applicable range and the economic feasibility, CAES is one of the most attractive candidates for MCT farm application in stand-alone islands.

Usually CAES plants use underground cavern to store compressed air [10]. Advanced adiabatic CAES (AA-CAES) concept was proposed to reduce the fossil fuel consumption in conventional CAES plants [11]. In AA-CAES, a thermal energy storage (TES) is used to absorb the compression heat during the charge process and release the heat to improve the energy density of the compressed air during the discharge process. An alternative concept of an ocean or underwater compressed air energy storage (OCAES or UWCAES) system was introduced by Seymour [12]. Anchored immersed-balloon or underwater open-ended containment structure is used for the air storage in OCAES. One dominant advantage of OCAES is that the air pressure in the tank is kept constant during the whole cycle, which avoids the exergy destruction of throttling happening in the conventional CAES [13]. Saniel et al. have proposed the conceptual design of an OCAES combined with TES in Ref. [14]. This conceptual OCAES is free from the geological limitation of the conventional cavern-based CAES and characterized by zero-emission as AA-CAES. The overall efficiency of this conceptual OCAES is up to 65.9%, which is close to the highest efficiency (70%) of an ideal AA-CAES.

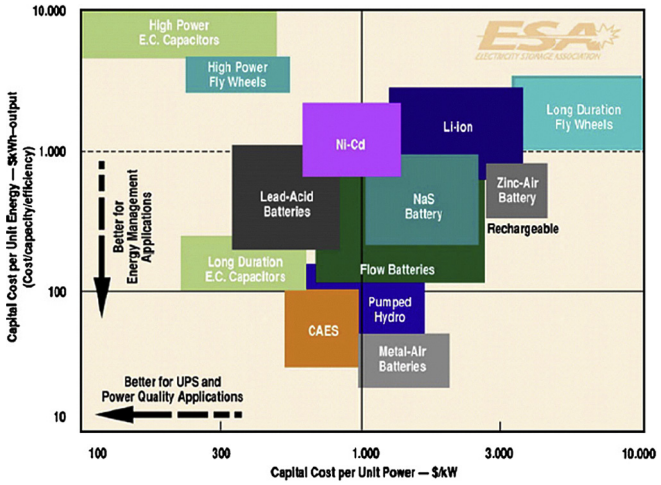

Fig. 1. Cost comparison of different energy storage systems [9].

In this work, a stand-alone island is considered. The island electricity consumption (load demand) is originally satisfied by the diesel generator (DG) systems. A hybrid OCAES/MCT/DG power supply system is proposed in this work to reduce DG fuel consumption. The original DGs become the backup power source and they will work only when MCT output power fails to meet the load demand. The subsystem modeling of each part will be presented in Section 2, and then the simulation results under different working cases are analyzed in Section 3, the conclusions and some discussions on the feasibility of CAES applications are given in Section 4.

2. Hybrid power system modeling

2.1. OCAES model parameters estimation

It is supposed that the stand-alone island has a base load with a peak power of 3 MW, and varies following a typical load curve [15,16]. For this typical load curve, the average and the minimum load values are 0.69 and 0.22 times the peak power respectively. Referring to the developed MCT model described in Ref. [6], 1.5 MW MCTs are considered in this paper. The daily tide velocity curve used in this work is shown in Fig. 2. We consider that the load demand takes up about 90% of the total generated power of the MCT farm considering some possible losses. In this case, 6 MCTs are required to supply the island. It is supposed that there is no mutual influence between each devices and the total MCT farm generated power is then considered to be 6 times of the single MCT power. Based on the above assumption, the power curves of the MCT farm and the load of this island are shown in Fig. 3.

For OCAES, an air compressor fulfills the charge process while an air turbine is used for the discharge process. Therefore, the rated charge and discharge powers are independent. This independence makes it flexible to determine the size of the compressor and air

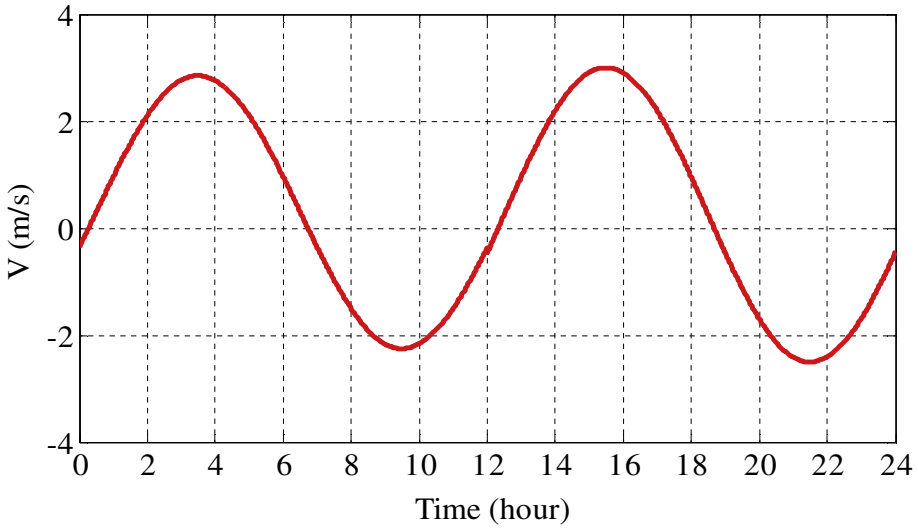

Fig. 2. Tide current speed during one day.

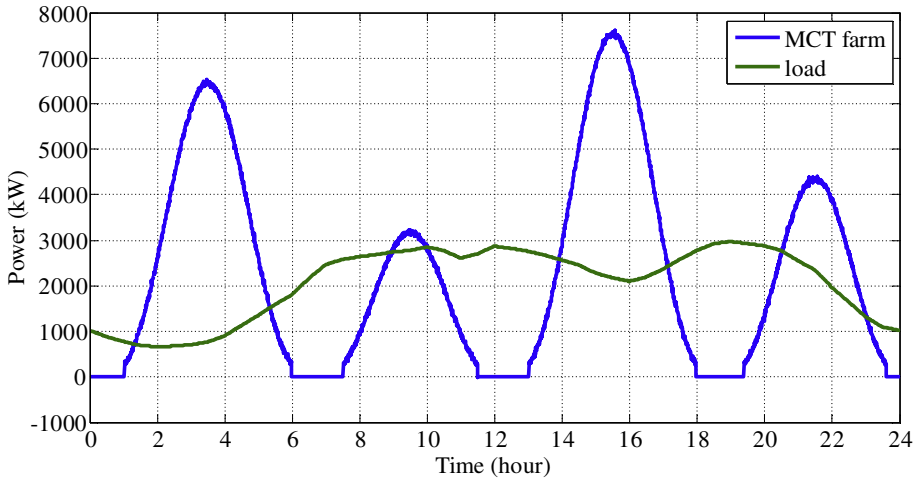

Fig. 3. Power curve of the studied MCT farm and load curve for a typical island in one day.

turbine. The difference between MCTs power and load (in Fig. 3) is the reference for determining the OCAES power rating. And, the integration of the power difference gives a rough estimation of the needed OCAES energy capacity.

In this paper, it is assumed that the charge power is positive and the discharge power is negative for the OCAES. It can be seen (from Fig. 4) that the maximum positive value of the difference is about 6 MW while the maximum negative value is about 3 MW. Therefore, the rated powers of the compressor and the gas turbine are designed to 6 MW and 3 MW respectively. It is assumed that the compressor and the gas turbine can work with the same efficiency at all the power range. From Fig. 4, the maximum value of the integration is about 13 MWh and the energy capacity of OCAES is then designed to be 15 MWh considering design margins.

2.2. OCAES modeling

OCAES is proposed to be combined with TES to increase the ESS efficiency. Based on the available literature [17–19], some assumptions are made as follows:

- The air is considered to be a binary ideal dry gas.
- 3-stage compressor with intercoolers and 3-stage air turbine with heaters are used. The compression and expansion are polytropic processes.
- The air storage is an ideal balloon, which can shrink totally during the discharge. No air leak happens in the air storage. The temperature of the air in the storage is same as that of the water, which is assumed to be 20 °C.
- TES is modeled as an ideal and simple module, subject to the classical heat transfer theory. Synthetic oil is used as the heat transfer fluid (HTF), and the specific heat capacity of the oil is close to that of the air.

During the charge, the air temperature will increase while the compressor compresses the air. Before entering the next stage, the air will be cooled by the intercooler with the heat being stored in the TES. It is noted that the maximum compressor outlet air temperature determines the temperature level of the TES. During the discharge, the air will expand and the air temperature decreases simultaneously; at the same time the heat from TES will heat the air. In order to prevent the air temperature dropping too low, the

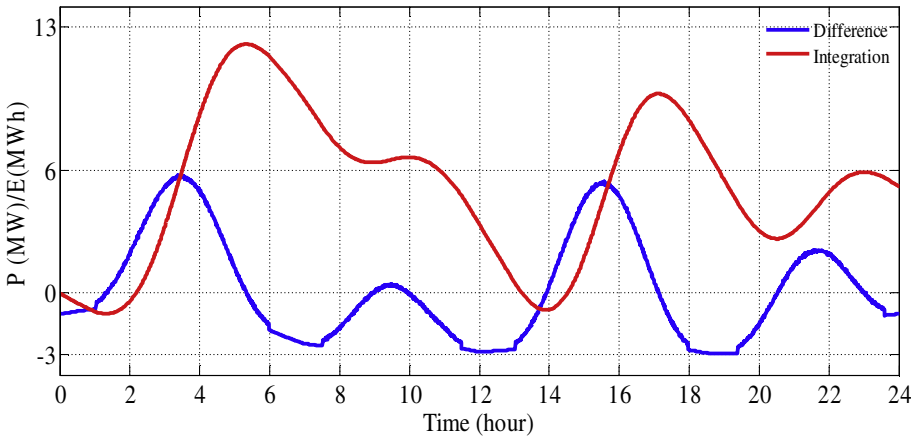

Fig. 4. Power difference ($P_{MCTs} - P_{load}$) and its integration.

pressure ratio in every stage of the air turbine should be properly set. In this work, the pressure ratio is set to the same value for all three stages. For the polytropic compression and expansion, the ideal gas follows the well-known polytropic equation and the ideal gas equation simultaneously.

$$pv^n = \text{constant} \tag{2}$$

$$pv = m_{air} R_a T \tag{3}$$

Based on these two equations, the outlet temperature of each stage in the compressor or turbine can be described by

$$T_{i,a}^{out} = T_{i,a}^{in} \beta_i^{(n-1)/n} \tag{4}$$

where β_i is the pressure ratio of each stage, it is equal to the ratio of the outlet pressure to the inlet pressure. The electricity consumed by each stage of compressor is calculated by Ref. [18].

$$P_{com} = \frac{1}{\eta_{m,c}} \dot{m}_{c,a} c_{p,a} \sum T_{ci,a}^{in} \left(\beta_{ci}^{(n-1)/n} - 1 \right) \tag{5}$$

where, $\eta_{m,c}$ is the mechanical efficiency of compressor, which is assumed to be constant. As for gas turbines, the generated power from air expansion is calculated by

$$P_{tur} = \eta_{m,t} \dot{m}_{t,a} c_{p,a} \sum T_{ti,a}^{in} \left(1 - \beta_{ti}^{(n-1)/n} \right) \tag{6}$$

where, $\eta_{m,t}$ is the mechanical efficiency of turbine; it is also assumed to be a constant.

The pressure in each stage is determined based on the pressure ratio setting, and the temperature determination in each stage is the critical issue for the calculation of the compression/expansion operation. A simplified ideal model is used for TES part. The TES is divided into the cold HTF storage and the hot HTF storage as shown in Fig. 5.

This model is similar to those proposed in Ref. [19]. During the operation, the temperatures of cold and hot HTF storage are supposed to be constant. The temperature of the cold HTF before entering the coolers is assumed to be 40 °C, while the average temperature of the compressor outlet air determines that of the hot HTF. Some simplifications are made: the hot fluid and cold fluid are supposed to exchange heat in a counter current type exchanger, and the heat is supposed to be transferred with a constant end temperature difference (20 °C) both in cold/hot side. In this way, the temperature of both air and the HTF in every stage of compressor and turbine can be determined.

For real application, a TES reservoir with large thermal capacity should be used. TES reservoir should be temperature stratified, in which the maximum and minimum temperatures are corresponding to the temperatures of hot and cold HTF in the simplified model. Fig. 6 shows the schematic diagram of the heat transfer for the equivalent conceptual TES reservoir. In order to determine the volume of the TES reservoir, the charge and discharge heat are calculated as follows [21,22].

$$\dot{Q}_{charge} = \dot{m}_{air} c_{p,a} \sum (T_{ci+1,0} - T_{ci,1}) \tag{7}$$

$$\dot{Q}_{discharge} = \dot{m}_{air} c_{p,a} \sum (T_{ti+1,0} - T_{ti,1}) \tag{8}$$

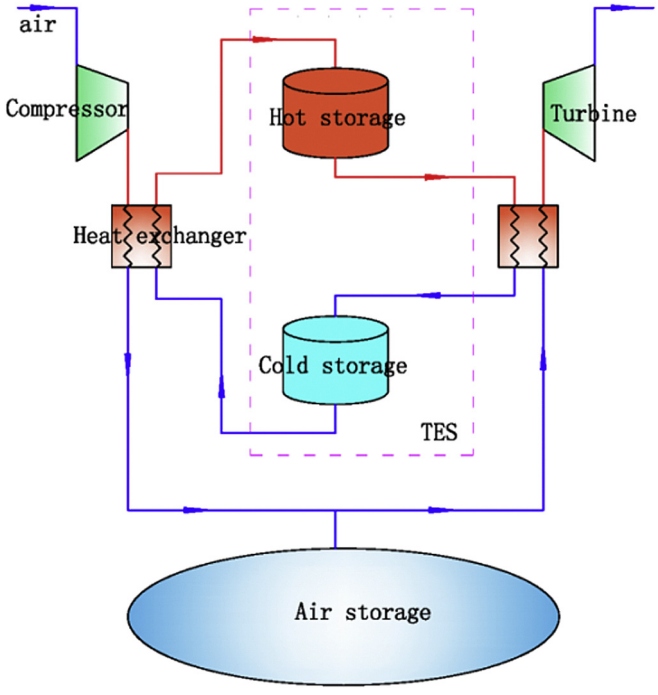

Fig. 5. Principle schema of an AA-OCAES.

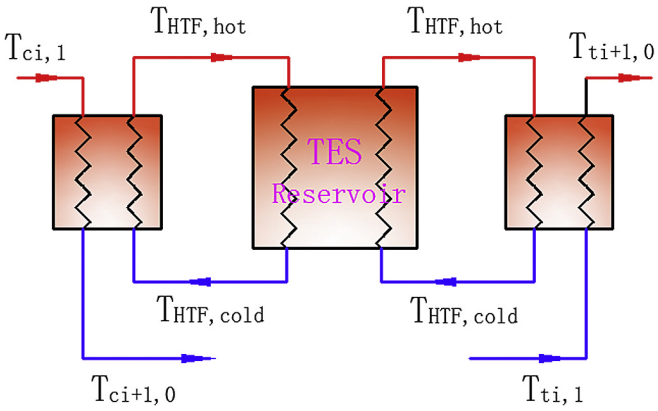

Fig. 6. Schematic diagram of the inner heat transfer for the OCAES [21].

2.3. OCAES charge and discharge tests

A charge/discharge test for the above OCAES model is carried-out: it will be charged for 2.5 h with the rated charging power of 6 MW, and then be discharged with the rated discharging power of 3 MW. The State of Charge (SoC) of the OCAES equals the volume ratio of the air left in the storage to the maximum volume of the container, which is also the mass ratio because of the constant pressure of the container. The SoC is then calculated by

$$SoC = \frac{\int_0^t \dot{m}_{air} dt}{m_{air,\max}} \tag{9}$$

The designed total air volume in the storage is calculated by

$$V_{air,total} = \frac{P_{charge} t_{charge} \eta_{m,c}}{c_{p,a} \sum T_{ci,a}^{in} \left(\beta_{ci}^{(n-1)/n} - 1\right)} \cdot \frac{R_a T_{ambient}}{p_0} \tag{10}$$

The designed volume of the TES reservoir is calculated by

$$V_{TES,reservoir} = \frac{Q_{charge} T_{charge}}{c_{p,TES}\left(T_{hot,HTF} - T_{cold,HTF}\right)} \tag{11}$$

The main parameters for the test of charge and discharge are listed the Appendix. The charge/discharge simulation results are shown in Fig. 7. The SoC increases from 0 to 1 after charging for 2.5 h, and then decreases to 0 after discharging for 3.03 h. Based on (12), the global efficiency of this OCAES is estimated about 60.6%. This efficiency is reasonable although it is a little higher than those of the existing developed CAES plant in McIntosh [14]. Calculated from (13), the heat recycle efficiency of TES is about 86.2%.

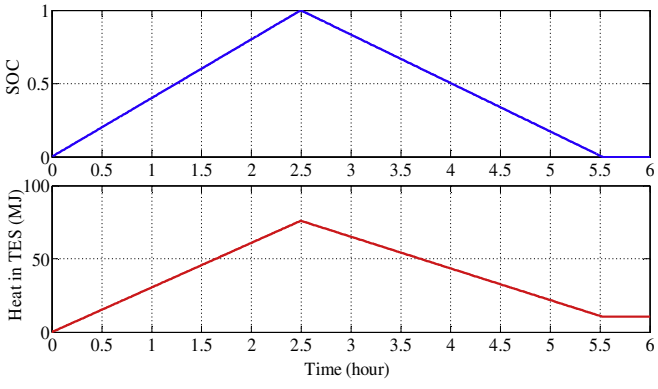

Fig. 7. Evolution of SoC and heat energy in TES reservoir during the charge-discharge tests.

$$\eta_{global} = \frac{P_{discharge} t_{discharge}}{P_{charge} t_{charge}} \tag{12}$$

$$\eta_{heat} = \frac{Q_{discharge} t_{discharge}}{Q_{charge} t_{charge}} \tag{13}$$

2.4. Hybrid OCAES/MCT/DG system modeling

The hybrid power system for the stand-alone island includes an MCT farm, an OCAES with TES and DGs. The power management issue of supply/demand balance during one or several days is concerned in this work. A simplified equivalent DC grid system is applied as shown in Fig. 8. The DC voltage source in Fig. 8 simulates the island load in the hybrid power system. This equivalent DC grid system facilitates simulations on a long-time scale. Indeed, using an equivalent DC grid allows studying the power fluxes without simulating finely the frequency and voltage control of the grid. The control design of the whole power system is aimed to utilize the renewable energy as much as possible to satisfy the load, and to maintain the grid balance between the supply and demand.

Adjusting the air mass flow controls the charging and discharging powers of the OCAES. This can be done by controlling the compressor and the turbine speed for a more detailed model. The charge/discharge power control scheme proposed in Ref. [6] is applied in this work. As shown in Fig. 9, the power reference of OCAES is determined by the difference between load and the power of MCT farm with respecting the OCAES limitations (the OCAES will be shut down if the SoC reaches 0 or 1).

It is assumed that there are multiple Diesel Generator sets with different rated powers that can run in parallel with high efficiency, and the total rated power of the DGs can meet the maximum load demand at any cases. DG control is directly linked to OCAES status. When the SoC of OCAES is lower than 0.05, DGs will start up. If the OCAES power reference is higher than the rated discharge power in some extreme cases, DG will operate to supply the load and keep OCAES power within its limitations.

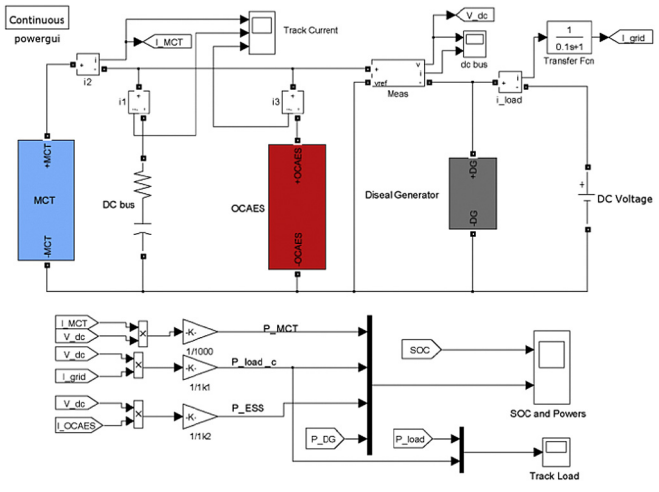

Fig. 8. Model of the hybrid power system in Matlab/Simulink.

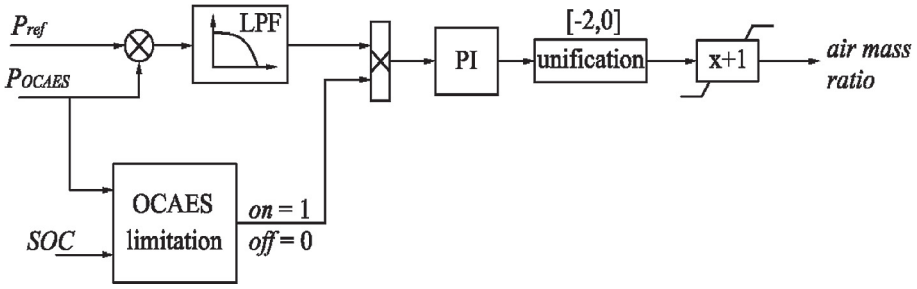

Fig. 9. OCAES control scheme.

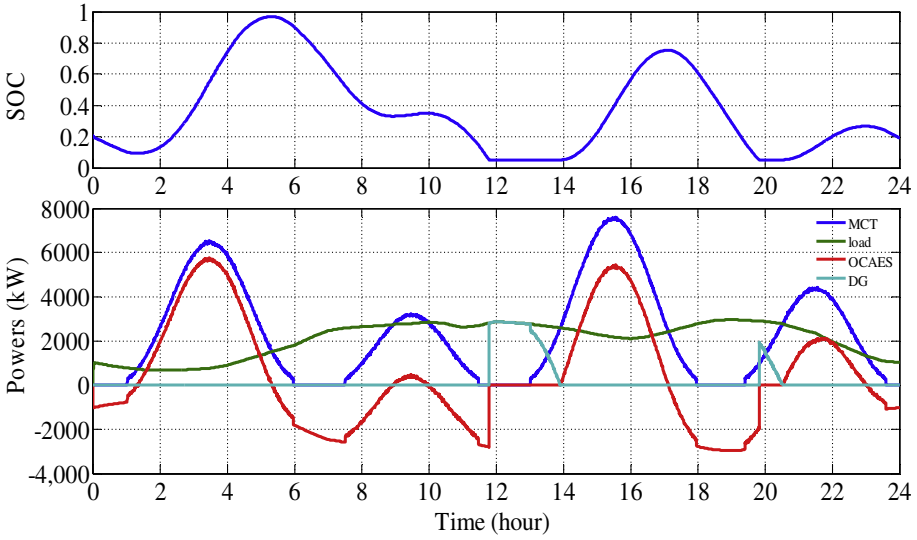

Fig. 10. Simulation results (SoC and powers) in the normal case.

3. Hybrid power system simulation in typical test cases

3.1. One-day normal case

In this case, it is supposed that the load and the tide velocity are varying under the designed conditions (as shown in Fig. 3). In this normal case, the initial SoC is set to 0.24. The simulation results of SoC and powers under this normal working condition are shown in Fig. 10.

The MCT farm operates in MPPT mode to maximize the power harnessed from the tidal currents. In the beginning, the load is supplied by OCAES because the current velocity is too low for MCT operation. With the increases of the tide velocity, the increasing power generated by MCT farm will meet the load demand and OCAES stops discharging. When the MCT power is higher than the load, the surplus power will be used to charge OCAES.

It can be calculated that DGs work for only 3 h in one day and contributes about 5.43 MWh to the load, which corresponds to about 10% of the total island load consumption. Therefore, the hybrid power system significantly helps reduce the fossil fuel consumption compared to conventional DG-supplied solutions. OCAES is charged and discharged alternately four times in one day. The maximum charge power is about 5.8 MW and the maximal discharge power is about 2.97 MW, so the chosen design options seem to be suitable for this test case. The maximum SoC of the ESS is about 0.97 and also reaches the lower limit sometimes. Although OCAES can be totally discharged theoretically, maintaining some remaining air in the balloon is good for the long service life. But the SoC is at a relatively high level at most time, which indicates that the volume design of air storage seems reasonable. The final SoC is 0.19 after working one day.

3.2. Higher or lower load cases

The load curve used in the normal case is the base load, which can be taken as the average case for this island. However, real daily load curve will vary for different periods. As an example, this load can vary strongly with working days or holydays or with seasonal

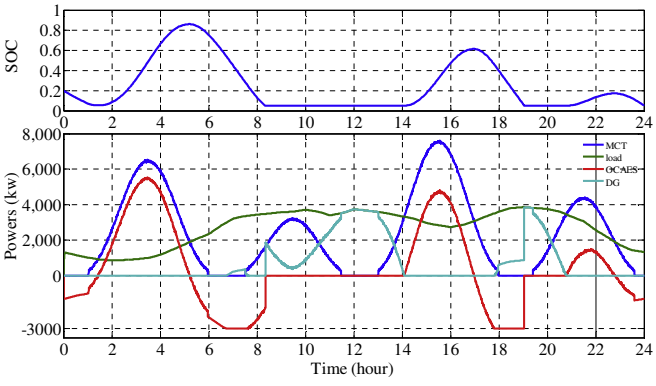

Fig. 11. Simulation results for the high load case (1.3 times normal load).

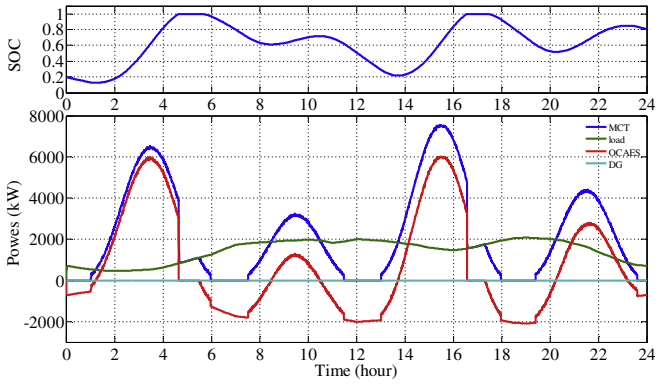

Fig. 12. Simulation results for the low load (0.7 times normal load).

consumer behavior. The higher load is set to be 1.3 times of the original normal load. The simulation results for this case are shown in Fig. 11. In this case, a remarkable increase of DG running time and contribution can be noticed. DGs contribute about 26.6% to the load during one day in this case, which is more than two times of the contribution in corresponding to the previous case.

The highest SoC of the OCAES attained in this case is only 0.87, and the SoC is at its lowest value for a long time. In addition, when OCAES reaches its rated discharge power at 6.74 h, DGs start up and assume the excess load. When SoC reaches its lower limit, OCAES stops discharging and DGs assume the main load with MCT farm. This case shows that DGs still play an important role for insuring the load following ability in the hybrid system, especially in high load cases.

The lower load case is carried out when the load demand is set to be 0.7 times of the original normal load. From Fig. 12, it can be found that OCAES is fully charged two times by the flooding tide. In order to maintain the grid stability, there is a sharp power decrease both for MCT farm and OCAES at 4.66 h and 16.57 h when OCAES was fully charged. One distinguished characteristic in this case is that the entire island load can be supplied by the joint operation of MCT farm and OCAES during this day and no DG operation (and consumption) is needed.

3.3. Higher or lower tide speed cases

The tidal current amplitudes vary with the relative position of the earth/moon/sun system (neap and spring tides). Fig. 13 shows the simulation results in the case where the tide speed increases by 10%. As it can be seen, OCAES will be quickly fully charged because of the high energy provided by the MCT farm. However, in this case, the MCT cannot be kept in MPPT operation when the OCAES charging power reaches its rated value at 2.69 h or 14.82 h; MCT control can limit the generated power to protect the OCAES from the over charge and maintain the stability of the grid [20]. When the OCAES is fully charged at 4.28 h or 16.81 h, the MCT limits the generated power to the load only. In this case, only about 4.1% of the island load is required to be supplied by DGs in one day.

A tidal cycle where the tide speed decreases by 20% is studied. As can be seen from Fig. 14, the highest SoC is 0.42 and it reaches the lower limit at most time of one day. Relatively, DGs work for the most time. It means that, the DG fuel consumption reduction is less efficient during a lower tidal speed cycle. In this case, the DGs are required to supply about 47.4% of the total load in the simulated day.

3.4. One-week case considering tidal amplitude variation

A simulation for one week has been carried out to observe the long-time operating performance of the proposed hybrid system and its control scheme. Based on the natural tidal speed variation phenomenon, it is assumed that the daily peak values of tidal current speed will decrease gradually by 30% during one week, while the load curve maintains about the same level for each day during this concerned week. The simulation results are shown in Fig. 15. From this figure, the load can be satisfied by the hybrid power source at anytime. The decay of the tide speed causes remarkable decrease of the generated power from the MCT farm.

The OCAES works at a low level of SoC in the last several days due to low availability of MCT farm output. At the same time, the requirement of DGs to supply the load increases at the end of the studied period when the tide amplitude becomes very low. This

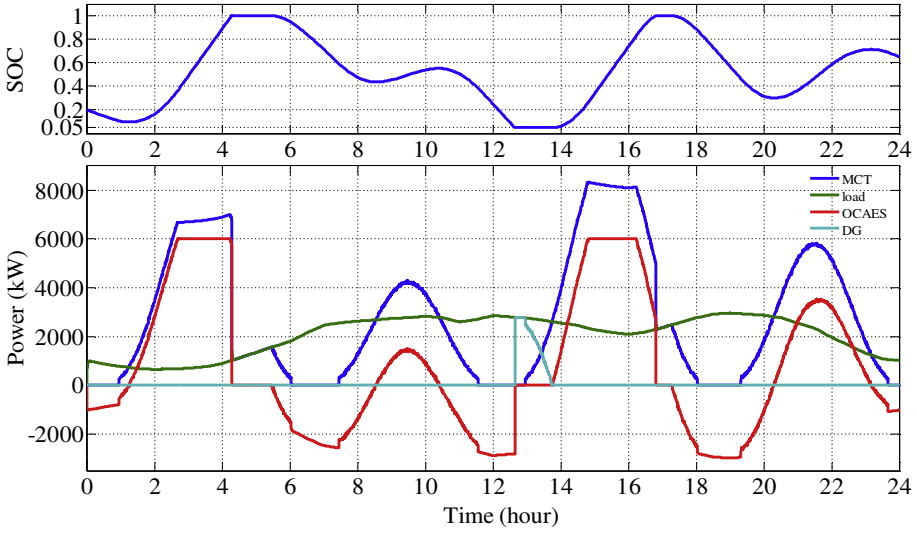

Fig. 13. Simulation results when the tide speed amplitude is increased by 10%.

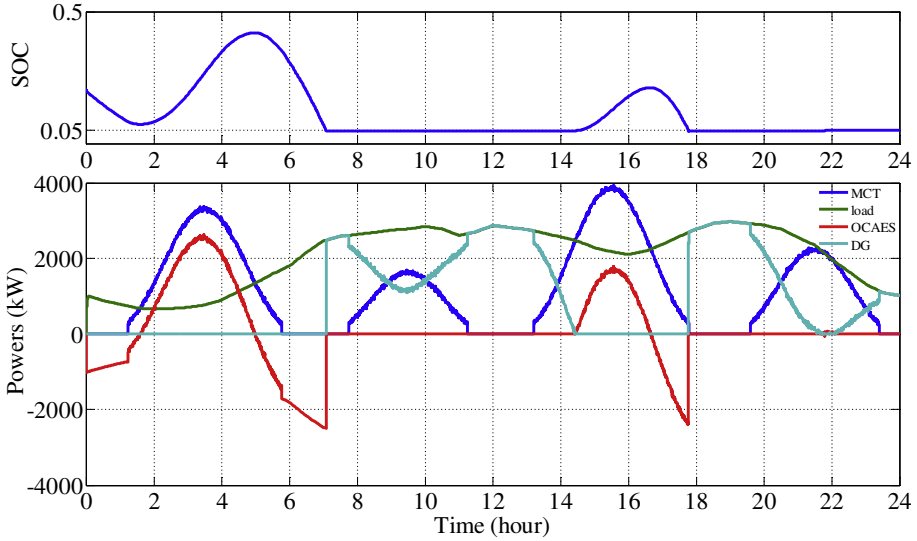

Fig. 14. Simulation results when the tide speed amplitude is decreased by 20%.

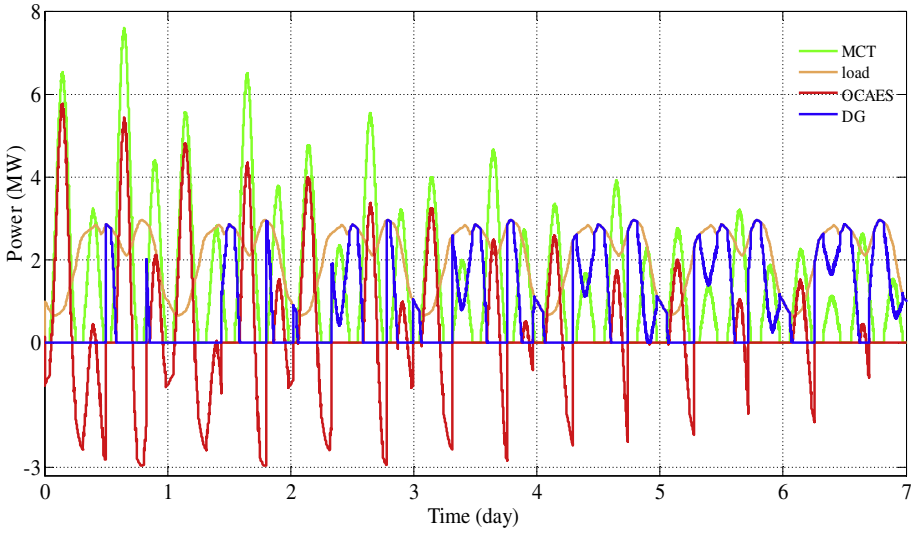

Fig. 15. Simulation results for the 7 days continuous operation.

makes DGs become the dominant power supply source at the end of the week. It can be calculated that DGs cover about 39.6% of the total island load consumption during the simulated week. In this case, the proposed hybrid power sources still allows reducing the fossil fuels by about 60% compared with conventional DG-based island power supply solution.

It should be noted that although the diurnal phase variations of the tidal speed (which could cause supply/load phase shift phenomenon) are not considered in the 7-days case simulation, the MCT farm output can be limited in case of extra MCT output reaching the rated OCAES power capacity in real application. Therefore, the OCAES would not need to be over-sized.

Table 1 summarizes the main simulation results of the different working condition. It is obvious that if DGs work longer in different one-day cases, it will contribute more to the load.

4. Conclusions and discussions

In this paper, a stand-alone island not connecting to the mainland grid is studied. The power supply system of this island is retrofitted from a conventional DGs set to a MCT-OCAES-DGs hybrid power system. The consumer power demand is assumed to be subject to a typical load curve. A MCT farm with six 1.5 MW turbines is considered as a renewable power supply source. A simplified OCAES model with TES was applied. Control strategies of the different subsystems were proposed and presented. Simulations were carried-out in different test cases to demonstrate the feasibility of the proposed hybrid power supply solution. Main achieved conclusions are as follows:

Table 1
Simulation results of different working cases.

Working conditions	DG/Load (%)	DG time(h)	Final SoC
Normal case[a]	10.9	2.8	0.19
1.3 *BL*[b]	26.6	9.6	0.05
0.7 *BL*	0	0	0.84
1.1 *BS*	4.1	1.1	0.7
0.8 *BS*	47.4	13.7	0.05
7-day case[c]	39.6	76.5	0.05

[a] Base Load (*BL*), Base Tidal Speed (*BS*), $SoC_0 = 0.24$, working in one day.
[b] Only one factor is changed in one-day cases.
[c] The tide speed decreases by 30% gradually in 7-day case.

– Load and tide speed have a significant impact on the contributions of the different power sources in the hybrid system.
– The tests for different cases validate the effectiveness of the proposed control strategy.
– The proposed hybrid system can provide a flexible power supply to the load in continuous operation even in extreme cases.

In most cases, cost-benefit assessments are major concerns before the final commercialization. The configuration of the hybrid system (power rating of single MCT and the total number of MCTs, OCAES sizing, DGs ratings and numbers) depends highly on the specific site conditions, load demand profiles, the costs (short-term and long-term) and the diesel-fuel consumption's reduction objective. The choice of CAES as the energy storage system relies on the fact that this technology offers the most economical solution for bulk energy storage: the cost of storage part (a priori between 40 €/kWh and 110 €/kWh for CAES) and annual operational and maintenance cost (4 €/kW) are the lowest compared with other energy storage technologies [23]. The cost-benefits analysis in Ref. [24] shows that the feasibility of the CAES plant strongly depends on the monthly payment from the regulating power market. Due to the predictability of the tidal current resource, integrating CAES in MCT farms could be more feasible than in the case of wind power systems. Different expander (energy generation capacity) and compressor (energy storage capacity) sizes, and system operational characteristics of the CAES can affect revenues and should be independently designed to optimize the economic benefits [25].

The optimal sizing of the power capacities of MCTs and OCAES system would be further studied taking into account of appropriate cost-evaluation models in the next step. It should be noted that optimal sizing of the elements in the hybrid MCT/OCAES/DG system is out of scope of this work, but it could be a very interesting study in the future.

Acknowledgment

The authors gratefully acknowledge the supports from French Navy Academy, France University of Brest, France and China-EU Institute of Clean and Renewable Energy, China.

Appendix

Table 2
OCAES main input parameters

n_c	1.5
n_t	1.33
$\eta_{m,c}$	0.92
$\eta_{m,t}$	0.92
$T_{ambient}$ (°K)	293
Pressure ratios of compressor	6, 2.6, 2.57
Pressure ratios of turbine	1/3.5, 1/3.5, 1/3.27
Cp_{air} (J/kg.k)	1003.5
Ra_{air} (J/kg.k)	286.7
ρ_{HTF} (kg/m^3)	570
Cp_{HTF} (J/kg.k)	1260
ρ_{TES} (kg/m^3)	2750
Cp_{TES} (J/kg.k)	916
Depth (m)	400
p_0 (bar)	40
Rating power (kW)	6000/3000
Charge time (h)	2.5
$T_{cold,\ HTF}$ (K)	313
V_{TES} (m^3)	121.4
$V_{air\ storage}$ (m^3)	2133

References

[1] K.W. Ng, W.H. Lam, K.C. Ng, 2002–2012: 10 years of research progress in horizontal-axis marine current turbines, Energies 6 (3) (2013) 1497–1526.
[2] Z. Zhou, F. Scuiller, J.F. Charpentier, M.E.H. Benbouzid, T. Tang, An up-to-date review of large marine current turbine technologies, in: Proceedings of the 2014 IEEE PEAC, Shanghai (China), November 2014, pp. 480–484.
[3] W.M.J. Batten, A.S. Bahaj, A.F. Molland, J.R. Chaplin, The prediction of the hydrodynamic performance of marine current turbines, Renew. Energy 33 (5) (May 2008) 1085–1096.
[4] M.H. Chiang, A novel pitch control system for a wind turbine driven by a variable-speed pump-controlled hydraulic servo system, Mechatronics 21 (4) (June 2011) 753–761.
[5] Z. Zhou, M.E.H. Benbouzid, J.F. Charpentier, F. Scuiller, T. Tang, A review of energy storage technologies for marine current energy systems, Renew. Sustain. Energy Rev. 18 (February 2013) 390–400.
[6] Z. Zhou, F. Scuiller, J.F. Charpentier, M.E.H. Benbouzid, T. Tang, Application of flow battery in marine current turbine system for daily power management, in: Proceedings of the 2014 IEEE ICGE, Sfax (Tunisia), March 2014, pp. 8–13.
[7] A.T. Jones, A. Westwood, Recent progress in offshore renewable energy technology development, in: Proceedings of the 2005 IEEE PESGM, vol. 2, June 2005, pp. 2017–2022. San Francisco (USA).
[8] US DOE, Ocean Energy Technology Overview, DOE/GO-102009-2823, July 2009.
[9] H. Ibrahim, A. Ilinca, J. Perron, Energy storage systems—characteristics and comparisons, Renew. Sustain. Energy Rev. 12 (5) (June 2012) 1221–1250.
[10] H.M. Kim, J. Rutqvist, D.W. Ryu, B.H. Choi, C. Sunwoo, W.K. Songa, Exploring the concept of compressed air energy storage (CAES) in lined rock caverns at shallow depth: a modeling study of air tightness and energy balance, Appl. Energy 92 (2012) 653–667.
[11] C. Bullough, C. Gatzen, C. Jakiel, M. Koller, A. Nowi, S. Zunft, Advanced adiabatic compressed air energy storage for the integration of wind, in: Proceedings of the 2004 EWEC, London (UK), November 2004.
[12] R.J. Seymour, Ocean energy on-demand using underocean compressed air storage, in: Proceedings of the 2007 OMAE, San Diego (USA), June 2007, pp. 527–531.
[13] A.J. Pimm, S.D. Garvey, M. de Jong, Design and testing of energy bags for underwater compressed air energy storage, Energy 66 (March 2014) 496–508.
[14] S.D. Lim, A.P. Mazzoleni, J. Park, P.I. Ro, B. Quinlan, Conceptual design of ocean compressed air energy storage system, in: Proceedings of the 2012 IEEE OCEANS, Hampton Roads (USA), October 2012, pp. 1–8.
[15] B. Wu, B. Zhang, J. Wang, J. Li, X. Zheng, Y. Liu, B. Mao, Y. Gao, Theoretical research for the application of flow storage battery in demand side management, in: Proceedings of the 2010 IEEE POWERCON, Hangzhou (China), October 2010, pp. 1–7.
[16] L. Sheng, Z. Zhou, J.F. Charpentier, M.E.H. Benbouzid, Island power management using a marine current turbine farm and an ocean compressed air energy storage system, in: Proceedings of the 11th European Wave and Tidal Energy Conference Series, Nantes (France), September 2015, pp. 1–6.
[17] D. Laing, W. Steinmann, R. Tamme, C. Richter, Solid media thermal storage for parabolic trough power plants, Sol. Energy 80 (10) (October 2006) 1283–1289.
[18] I. Arsie, V. Marano, G. Nappi, G. Rizzo, A model of a hybrid power plant with wind turbines and compressed air energy storage, in: Proceedings of the 2005 ASME Power Conference, Chicago (USA), April 2005, pp. 987–1000.
[19] A. Gil, M. Medrano, I. Martorell, A. Lazaro, P. Dolado, B. Zalba, L.F. Cabeza, "State of the art on high temperature thermal energy storage for power generation. Part 1—concepts, materials and modelization, Renew. Sustain. Energy Rev. 14 (January 2010) 31–55.
[20] Z. Zhou, F. Scuiller, J.F. Charpentier, M.E.H. Benbouzid, T. Tang, Power control of a non-pitchable PMSG-based marine current turbine at over-rated current speed with flux-weakening strategy, IEEE J. Ocean. Eng. 40 (3) (July 2015) 536–545.
[21] F. de Samaniego Steta, Modeling of an Advanced Adiabatic Compressed Air Energy Storage (AA-CAES) Unit and an Optimal Model-based Operation Strategy for its Integration into Power Markets, Master Thesis, Swiss Federal Institute of Technology, Zurich, October 2010.
[22] N. Hartmann, O. Vöhringer, C. Kruck, L. Eltrop, Simulation and analysis of different adiabatic compressed air energy storage plant configurations, Appl. Energy 93 (May 2012) 541–548.
[23] B. Zakeri, S. Syri, Electrical energy storage systems : a comparative life cycle cost analysis, Renewable and Sustainable Energy Reviews 42 (February 2015) 569–596.
[24] H. Lund, G. Salge, The role of compressed air energy storage (CAES) in future sustainable energy systems, Energy Convers. Manag. 50 (5) (May 2009) 1172–1179.
[25] E. Drury, P. Denholm, R. Sioshansi, The value of compressed air energy storage in energy and reserve markets, Energy 36 (5) (August 2011) 4959–4973.